Indonesian Journal of Electrical Engineering and Informatics (IJEEI)
Vol. 9, No. 3, September 2021, pp. 615~632
ISSN: 2089-3272, DOI: 10.52549/ijeei.v9i3.3009

Novel application of Selfish Herd Optimisation based fractional order cascaded controllers for AGC study

Subhadra Sahoo[1], Narendra Kumar Jena[2], *Binod Kumar Sahu[3], Prakash Kumar Ray[4]
[1,2,3]Department of Electrical Engineering, ITER, Siksha O Anusandhan University, Bhubaneswar, Odisha, India.
[4]College of Engineering and Technology, Bhubaneswar, Odisha, India

Article Info

Article history:

Received Feb 11, 2021
Revised Aug 1, 2021
Accepted Aug 29, 2021

Keyword:

Automatic Generation Control
2-Degrees of Freedom
Two-stage controller
Fractional order Controller
Selfish Herd Optimization

ABSTRACT

In a modern, and complex power system (PS), robust controller is obligatory to regulate the frequency under uncertain load/parameter change of the system. In addition to this, presence of nonlinearities, load frequency control (LFC) of a Power System becomes more challenging which necessitates a suitable, and robust controller. Single stage controller does not perform immensely against aforesaid changed conditions. So, a novel non-integer/fractional order (FO) based two-stage controller incorporated with 2-degrees of freedom (2-DOF), derivative filter (N), named as 2-DOF-FOPIDN-FOPDN controller, is adopted to improve the dynamic performance of a 3-area power system. Each area of the power system consists of both non-renewable and renewable generating units. Again, to support the superior performance of 2-DOF-FOPIDN-FOPDN controller, it is compared with the result produced by PID, FOPID, and 2-DOF-PIDN-PDN controllers. The optimal design of these controllers is done by applying Selfish Herd Optimisation (SHO) technique. Further, the robustness of the 2-DOF-FOPIDN-FOPDN controller is authenticated by evaluating the system performance under parameter variation. The work is further extended to prove the supremacy of SHO algorithm over a recently published article based on pathfinder algorithm (PFA).

Corresponding Author:

Binod Kumar Sahu,
Department of Electrical Engineering, ITER,
Siksha O Anusandhan University, Bhubaneswar, Odisha, India.National Chung Cheng University,
Email: binoditer@gmail.com

1. INTRODUCTION

The modern power system becomes nonlinear, bulky and more complex, to satisfy the continuous increase in load demand. The performance of such interconnected power system is mostly affected by the random load change and uncertainties of parameters. Hence, it becomes a challengeable task to maintain the reliability and stability of the electric PS. The system stability depends upon the balance between total power generated by the synchronous generators and the total load demand. Since, the load demand varies randomly with the time, the frequency of the system along with the tie line power starts deviating from their nominal values. Automatic generation control (AGC) helps to maintain the power balance in the wake of perturbation of load by which area frequency and tie line power remains unaltered. In each area if the AGC is incapable to handle the excursion of frequency and power in the tie line within the predefined acceptable limit, then the stability of the power system gets worsen [1] culminating a possibility of blackout. Hence, AGC in a complex system becomes one of the crucial issues of a PS.

For the frequency and tie-line power stability, different power system models are considered and the load frequency control (LFC) of these PSs are studied by different Researchers as presented below. Ramakrishna et al. [2] demonstrated conventional proportional-integral (PI) controller for the AGC of a single area multi source PS. Dabur et al. [3] studied both AGC and automatic voltage regulator (AVR) of single area thermal

system. Kothari et al. [4] analysed the discrete mode AGC for a two-area interconnected PS comprising reheat thermal PS. LFC of a two-area hydro thermal system is studied by Bhise et al. [5]. Many researchers gradually introduced various non-linearities such as generation rate constraint (GRC), governor dead band (GDB), time delay and boiler dynamics in to the power system to make the system more realistic. Subha [6] has taken an attempt to study the AGC of an interconnected PS by including both GRC and GDB as nonlinearities. Tripathy et al. [7] analysed LFC in a two-area power system including GRC, GDB and Boiler dynamics. Gozde et al. [8] have cited the effect of GDB with GRC in a two-area thermal system. Guha et al. [9] explored a two-area system, each area carrying three sources and presented the LFC of that system employing GRC, GDB and Boiler dynamics. Load frequency control (LFC) in an unequal three area having thermal units employing the GRC is explained by Nanda et al. [10].

Controller design is a key problem to enhance the performance of LFC. The conventional PID controller is the primary and earlier controller which has been attempted by various researchers to study the LFC of power system. In the beginning, Elgerd and Fosca [11] introduced the concept of integral (I) controller for the load frequency control of a PS. Parmer et al. [12] demonstrated PI controller for the AGC of an interconnected power system. Ali et al. [13] recommended PID controller for the LFC of hydro power plant. With increase in non-linearities of the system, artificial intelligence-based controller replaced the conventional PID controller to improve the frequency stability. The fuzzy PI controller is considered by Sahu et al. [14] to deal AGC issues in multi area system. Sahu et al. [15] implemented fuzzy-PID controller to study the dynamic behaviour of AGC system. Adaptive fuzzy PID controller is demonstrated by Sahoo et al. [16] for the LFC of a restructured power system. Despite all the advantages of the aforementioned controllers, we can't avoid the classical controller completely because of its robustness and simplicity. Hence, different features are added with the classical controller, to enhance its performance. A 2-DOF PID controller is deployed by Sahu et al. [17] to study the LFC of a two-area system considering GDB. Nayak et al. [18] employed 2-DOF based fuzzy PID controller to improve the stability of an interconnected power system. Morsali et al. [19] proposed the FOPID controller to improve the performance of AGC in a multi area system. Farook et al. [20] proposed fractional order PID controller for frequency stability of a deregulated system. A two-stage controller named PD-PID cascaded controller is employed by Dash et al. [21] to enhance the stability of a multi area thermal system. Cascaded PD-PID controller with filter coefficient is proposed for the AGC of a multi area interconnected power system by Debnath et al. [22]. Saha and Saikia [23] precisely presented a fractional order cascade controller to carry the AGC study in a restructured environment. Recently, Tasnin et al. [24] have proposed a FOPI-FOPD controller to compare the performance of AGC system with different energy storage devices. Arya et al. [25] suggested the cascaded non-integer controller for AGC of hydro-thermal power system with renewable sources. A 2-DOF-PI-FOPDN controller is recommended by Prakash et al [26] for the LFC of a multi-source interconnected power system having HVDC link. Sitikantha et al. [27] proposed 2-degree of freedom FOPID controller to enhance the dynamic performance of an interconnected system. Raj and Shankar [28] combined 2-DOF PID controller with fractional order (FO) ID controller for LFC of a three area multi source restructured system. A 3-DOF non-integer/FO controller cascaded with PD controller is proposed by Jena et al. [29] for a two-area interconnected system.

Selection of the gain parameters of the controllers play prime role for the better performance of the controllers. Hence several computational algorithms such as genetic algorithm (GA) [2], particle swarm optimisation (PSO) [8], bacteria foraging algorithm [10], symbiotic organism search algorithm [9,18], hybrid of PSO and pattern search algorithm [14], teaching learning based optimisation [15], differential evolution [17], hybrid of GA and fire-fly [20], whale optimisation [23, 27], sine-cosine algorithm [25], flower pollination algorithm [21], interactive search algorithm [28], wild goat algorithm [29], grey wolf optimisation technique [30] etc. applied for tuning of the controller gains. A new computational algorithm named selfish herd optimisation (SHO) developed by Fausto et al. [31], is adopted in this work to design optimally the gains of some conventional and cascaded controllers.

To ascertain, the improvement in system specification such as undershoot, overshoot and settling time, the time response is imposed to an objective function. Bhise et al. [5] taken integral square error (ISE) as objective function. The objective functions ISE and integral time square error (ITSE) are chosen to design the controllers' gains by Magid and Abido [32]. Gozde et al. [33] taken integral absolute error (IAE), ITSE, ISE and integral time absolute error (ITAE) as objective functions to optimise PI and PD controller gains by artificial bee colony (ABC) algorithm.

Main contributions of this paper:

a. A 3-area multi-source PS, is modelled in MATLAB/SIMULINK platform and GRC, GDB and boiler dynamics are introduced as the non-linearities to realize a realistic power system.
b. To obtain better performance of the AGC of the above system, a novel 2-DOF-FOPIDN-FOPDN cascaded controller is developed.

c. An efficient computational optimisation algorithm, SHO is used for optimising the gains of these controllers.
d. The result of 2-DOF-FOPIDN-FOPDN cascaded controller is compared with that of PID, FOPID, and 2-DOF-PIDN-PDN controllers from which 2-DOF-FOPIDN-FOPDN cascaded controller is proved to be superior.
e. Robustness analysis of the proposed controller is done by providing random load variations and also by varying system parameters.
f. This work is extended to prove the supremacy of the applied optimisation technique and the proposed controller by comparing its result with that of a recently addressed work [34], considering a two-area hydro-thermal-gas system

The remaining part of the paper is organized as follows. Section 2 includes the linearised model of the proposed system. Section 3 explains the proposed controller and some of its counterparts in details. Section 4 describes the selection of objective function to optimally design the controllers. SHO optimisation technique is described in the section 5. Simulation results and discussions under various conditions are illustrated in section 6. An extended work is included in section 7 to prove the efficacy of SHO algorithm over pathfinder algorithm. Section 8 ascribes conclusion of the proposed study observing sections 1 to 7.

2. POWER SYSTEM MODEL

The transfer function model of a three-area multi source PS is shown in Figure 1.

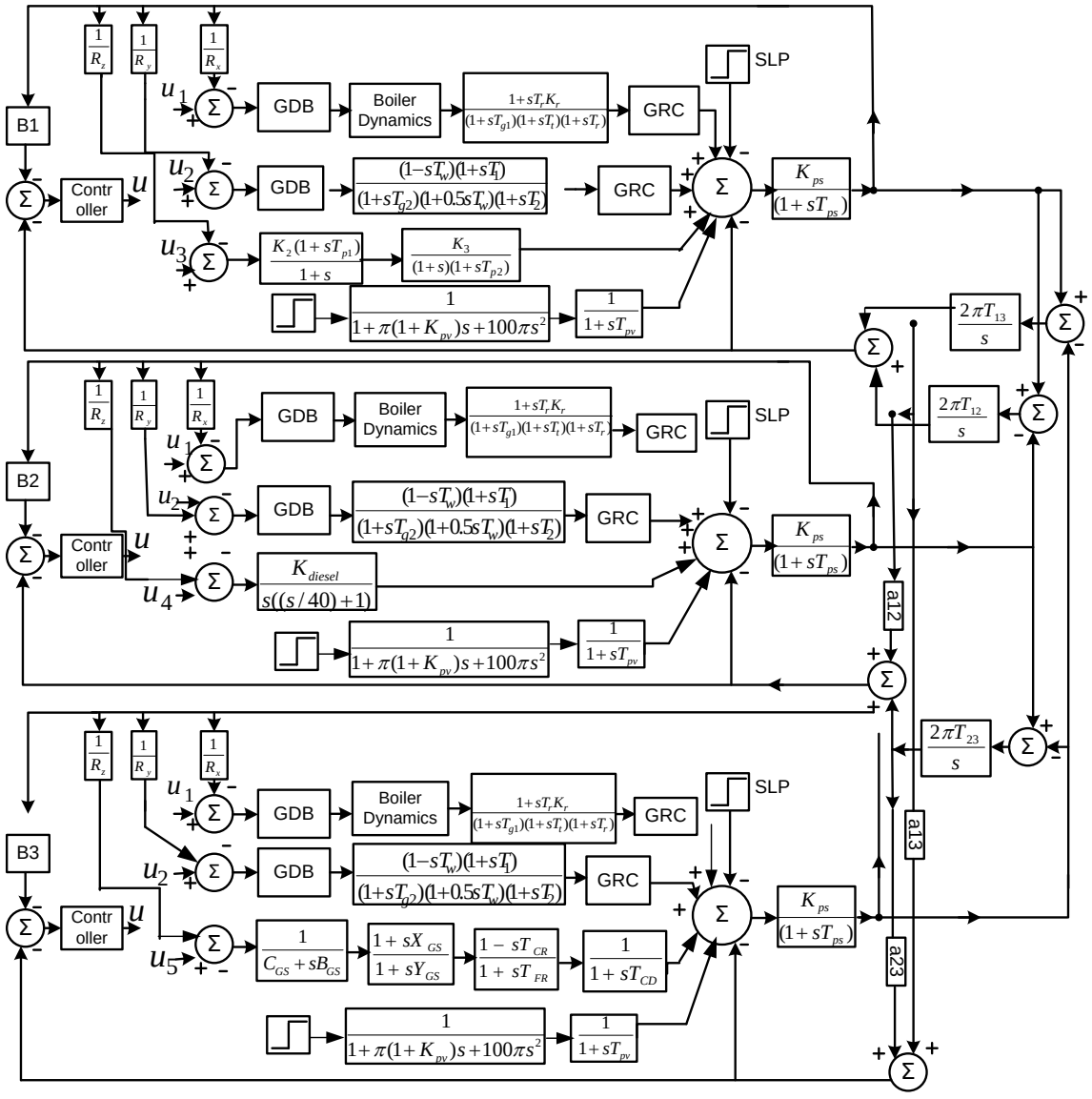

Figure 1. Model of three area system

Each area of the power system consists of four different generating units. Area-1 is equipped with a thermal unit, a hydro unit, a wind farm and a solar unit. Area-2 is having a diesel unit along with hydro-thermal units and solar power plant. Area-3 is integrated with a diesel unit, a solar unit in addition to hydro-thermal units. Hydro and thermal generating units of all the areas are subjected to nonlinearities such as GRC, GDB and boiler dynamics. The gain parameters of hydro and thermal units are taken from reference [15]. Linearized mathematical modelling of gas unit, GRC for both hydro & reheat thermal units and GDB are taken from Morsali et al. [35]. To make the power system more practical, boiler dynamics for thermal units is considered by referring the article published by Tripathy et al. [7]. Linearized transfer function models of wind farm and diesel unit are taken from from Guha et al. [9]. The solar system parameters are taken from [36].

2.1. Boiler System

In thermal power system, Boiler dynamics is taken into consideration because the fuel and steam flow for the active power balance affects the boiler pressure. In this study drum type boiler is used which helps in separating steam water from steam and then feeds the steam to the super heater. Transfer function model of boiler dynamics is shown in Figure 2 (a).

2.2. Generation Rate Constraint (GRC)

GRC is the limit on the rate of change of generated power because of the turbine of the synchronous generator [9]. For the thermal and hydro power plants this constraint is unavoidable in LFC study. For raising and lowering the power generation of hydro generating units, GRC of 270%/min and -360%/min are considered respectively. Whereas, GRC of ± 3%/min is considered for thermal generating units. Transfer function block of GRC is depicted in Figure 2 (b).

2.3. Governor dead band (GDB)

It is the total magnitude of change in speed without alteringg the valve position. The describing function which has a sustained oscillation with natural frequency $f_0 = 0.5Hz$ is defined as:

$$y = f(x, x') \quad (1)$$

$$x = M\sin(\omega_0 t) \quad (2)$$

Where M is amplitude and $\omega_0 = 2.\pi.f_0$ is natural angular frequency. Fourier expansion of equation (2) is

$$f(x, x') = F^0 + N_1.x + \frac{N_2}{\omega_0}.x' + ... \quad (3)$$

Considering the backlash as symmetrical about the origin i.e., $F^0 = 0$, the approximation of the above function is minimised as given in equation (4).

$$f(x, x') = N_1.x + \frac{N_2}{\omega_0}.x' = \left(N_1 + \frac{N_2}{\omega_0}.\frac{d}{dt}\right)x = DB.x \quad (4)$$

Where, DB is the dead band. In this study, a back lash of 0.05% is taken [7]. Here, $N_1 \& N_2$ are taken as 0.8 and -0.2 respectively.

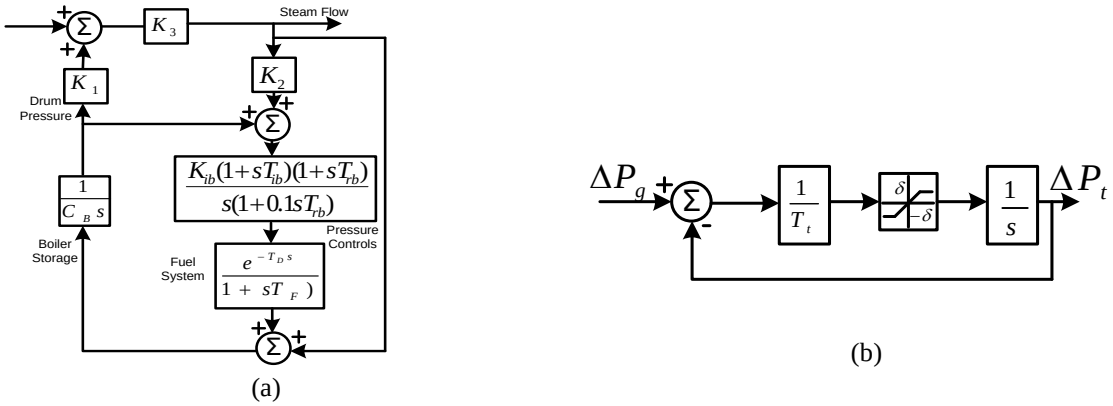

Figure 2. (a) Boiler dynamics model, (b) GRC dynamic model.

3. RESULTS AND ANALYSIS

3.1. PID controller

PID controller is the combination of Proportional, Integral and Derivative controllers. It is the most robust, simple and reliable controller. Hence, it is the most popular controller industries. Superiority of PID controller is proved over PI and I controllers in many literatures. Figure 3 (a) shows the structure of the PID controller. Its transfer function is expressed as:

$$\frac{U(s)}{E(s)} = k_p + \frac{k_i}{s} + k_d.s \tag{5}$$

Where, $k_p, k_i, \& k_d$ are the gains.

3.2. *Fractional order controller*

The concept of fractional order controller is based upon differential equations using fractional calculus. The fractional calculus widens the area of integer order controller. The $PI^{\sigma}D^{\zeta}$ controller is first implemented in power system by Podlubny [37], in which the integrator and differentiator are of non-integer order. Though there are five parameters to be optimized, fractional order makes it more flexible and robust. The non-integer calculus for integration and differentiation is given as:

$$a^{D_t^q} = \begin{cases} \dfrac{d^q}{dt^q}, q > 0 \\ 1, q = 0 \\ \displaystyle\int_a^t (d\tau)^{-q}, q < 0 \end{cases} \tag{6}$$

Caputo form of solution of equation (6) given by:

$$a^{D_t^q} f(t) = \begin{cases} \dfrac{1}{\Gamma(m-q)} \displaystyle\int_a^t \frac{f^{(m)}(\tau)}{(t-\tau)^{q+1-m}} d\tau & ; m-1 < q < m \\ \dfrac{d^m}{dt^m} f(t) & ; q = m \end{cases} \tag{7}$$

Where, Γ is a Gamma function and m is a first integer greater than q. Laplace transformation (7) is:

$$L\left(0^{D_t^q} f(t)\right) = s^q F(s) \tag{8}$$

To obtain the solution of a non-integer based differential equation, numerical approximation method may be adopted. By Oustaloup approximation method [38], equation (8) can be written as:

$$s^q = K \prod_{n=1}^{N} \frac{1 + \dfrac{s}{\omega_{zn}}}{1 + \dfrac{s}{\omega_{pn}}} \qquad ; q > 0 \tag{9}$$

In equation (8), there are N number of poles and zeros for which approximation is considered between the frequencies ω_l and ω_h. K is a gain of the function. N is chosen such that ripples in gain and phase is smaller and approximation is less difficult. Frequency of poles and zeros are given as follows:

$$\omega_{z,1} = \omega_l.\sqrt{n} \tag{10}$$

$$\omega_{p,n} = \omega_{z,n}.\varepsilon \tag{11}$$

$$\omega_{z,n+1} = \omega_{p,n}\sqrt{\eta} \tag{12}$$

$$\eta = \left(\frac{\omega_n}{\omega_l}\right)^{(1-q)/N} \tag{13}$$

$$\varepsilon = \left(\frac{\omega_h}{\omega_l}\right)^{q/N} \tag{14}$$

In the above expression if $|q>1|$, the Oustaloup estimation may not fit well as it makes the term s^q rational. therefore, the power of complex frequency is decomposed as:

$$s^q = s^n s^\sigma \tag{15}$$

Where $n \in z$ and $q = n+\sigma$.

Here s^σ is to be estimated. In this study, 0.01 rad/s and 100 rad/s are taken as the lower and upper corner frequencies respectively [38].

It is clear from Figure 3 (b), that FOPID controller can satisfactorily perform on the whole plane whereas, its conventional PID works only at defined points. This makes the FOPID controller to perform efficiently with systems having more nonlinearity. The FOPID controller has five parameters namely, k_p, k_d, k_d, ζ and σ The $PI^\sigma D^\zeta$ is the simplest non-integer order controller, where, σ and ζ are the fractional order parameters. From the Figure 3 (c), it is clear that, the transfer function of FOPID controller is given as:

$$\frac{U(s)}{E(s)} = k_p + \frac{k_i}{s^\sigma} + k_d s^\zeta \tag{16}$$

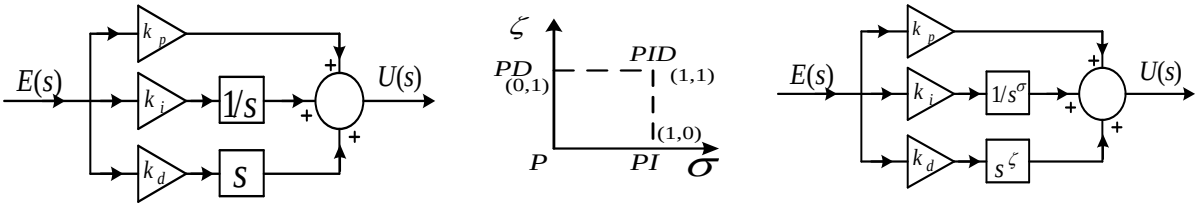

Figure 3. (a) PID control structure, (b) FO controller working Range, (c)FOPID control structure.

3.3. *Cascade controller*

Generally, in a non-linear system, the PID controllers may not provide satisfied result. Hence classical PID controllers are modified in different manner to reduce the frequency deviation. Cascaded controllers (conglomerating PID and its variants) are one of them. The PI controller is connected in cascade with PD controller with filter in derivative part (PI-PD controller) to deal with AGC issues in a multi area power system by Pan et al. [39]. Here to study AGC of the proposed three-area system PIDN controller is cascaded with PDN controller having two-degree of freedom (2-DOF-PIDN-PDN). Again, the study is further extended to design a novel cascaded controller by incorporating fractional integro-differential operator and two-degree of freedom, called 2-DOF-FOPIDN-FOPDN controller. The $PI^\sigma D^\zeta$ controller is kept in the inner loop and PD^ζ the controller is kept in outer loop. Hence the error signal is controlled in two different stages instead of single stage. Structure of a cascaded controller with 2-DOF is depicted Figure 4 (a) and its transfer function in Laplace domain is given in equation (17). The 2-DOF FOPIDN-FOPDN controller is given in the Figure 4 (b).

$$\begin{aligned} Y(s) = &\left(\frac{g_1(s).g_1(s).c_1(s).c_2(s)}{1+g_2(s).c_2(s)+g_1(s).g_2(s).c_1(s).c_2(s)} \right).r(s) \\ &+ \left(\frac{g_1(s)}{1+g_2(s).c_2(s)+g_1(s).g_2(s).c_1(s).c_2(s)} \right).d_1(s) \end{aligned} \tag{17}$$

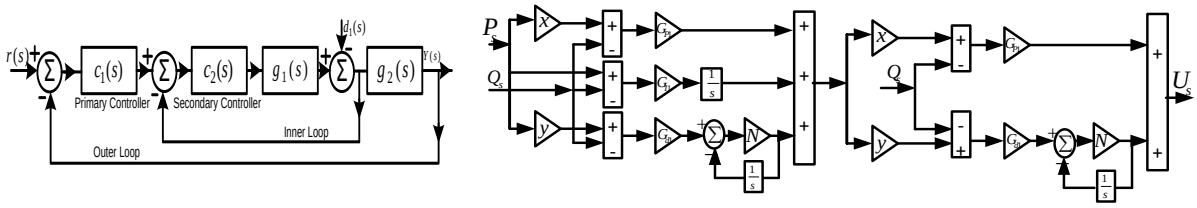

(a) (b)

Figure 4. (a) 2-DOF cascaded controller structure, (b) Control structure of 2-DOF-FOPIDN-FOPDN.

Transfer function of $PI^\sigma D^\zeta N$ controller is given as:

$$X_1(s) = G_p + \frac{G_i}{s^\sigma} + G_d s^\zeta \left(\frac{N_f}{N_f + s^\zeta} \right) \quad (18)$$

Similarly, for $PD^\zeta N$ controller the transfer function is:

$$X_2(s) = G_p + G_d s^\zeta \left(\frac{N_f}{N_f + s^\zeta} \right) \quad (19)$$

From Figure 4 (b), output of the first stage controller can be written as:

$$X(s) = \left[x.G_p + \frac{G_i}{s^\sigma} + y.G_d.s^\zeta \left(\frac{N_f}{N_f + s^\zeta} \right) \right].P(s) + \left[G_p + \frac{G_i}{s^\sigma} + G_d.s^\zeta \left(\frac{N_f}{N_f + s^\zeta} \right) \right].Q(s) \quad (20)$$

Similarly, the transfer function of the controller shown in fig. 4 (b) can be written as:

$$U(s) = X(s).\left[x^{'}.G_p + \frac{G_i}{s^\sigma} + y^{'}.G_d.s^\zeta \left(\frac{N_f}{N_f + s^\zeta} \right) \right] + Q(s).\left[G_p + G_d.s^\zeta \left(\frac{N_f}{N_f + s^\zeta} \right) \right] \quad (21)$$

4. MATHEMATICAL PROBLEM FORMULATION

To carry out the AGC study, a 3-area power system, each area having four sources is considered as shown in Figure 1. Four different controllers such as PID, FOPID, 2-DOF-PIDN-PDN, 2-DOF-FOPIDN-FOPDN are implemented for reducing the frequency and power deviations in the tie-line. For five different kinds of sources, present in different control areas, five controllers are used as the secondary controllers for the stability of the power system. The gain parameters of the controllers are tuned by a recently developed SHO algorithm. A step load change of 1% is applied in the first area to study the dynamic stability of the proposed system. To establish better control, a time domain integral performance index ITAE is chosen as its performance in terms of settling time, overshoot and undershoot, out plays other indices such as ITSE, IAE and ISE. The ITAE is expressed in equation (22).

$$J = \int_0^T t \left[|\Delta f_1| + |\Delta f_2| + |\Delta f_3| + |\Delta p_{tie12}| + |\Delta p_{tie23}| + |\Delta p_{tie31}| \right] dt \quad (22)$$

The objective function 'J' is minimised through optimisation technique to determine the optimal controllers' gains, subjecting to the following constraints:

$G_{p,min} \le G_p \le G_{p,max}$, $G_{i,min} \le G_i \le G_{i,max}$, $G_{d,min} \le G_d \le G_{d,max}$, $\sigma_{min} \le \sigma \le \sigma_{max}$, $\zeta_{min} \le \zeta \le \zeta_{max}$, $F_{min} \le F \le F_{max}$.

Where, $G_{pid,\min}$ and $G_{pid,\max}$ are taken in between 0.01 and 5, $\sigma_{FOPID,\min}$ and $\sigma_{FOPID,\max}$ are chosen in between 0.01 and 1, $\zeta_{FOPID,\min}$ and $\zeta_{FOPID,\max}$ are selected in the within the range [0 1], and the filter coefficients (N_f) are chosen in between [20-200]. Weighting parameters of 2-DOF cascaded controller such as x, $x^{'}$, y and $y^{'}$ are taken in the range of [0 1]. The aforementioned gains are optimally designed by SHO algorithm.

5. OPTIMISATION TECHNIQUE: SELFISH HERD OPTIMIZATION (SHO)

Fausto et al. [31] developed Selfish Herd Optimizer (SHO) as an efficient, bio-inspired algorithm for global optimization, which is based upon the selfish herd theory as described by Hamilton (1971). This theory describes predatory interactions between two groups of animals. The two groups are (a) Prey (b) Predator. Each prey moves one position to another to escape themselves from the hungry predators. The prey with maximum survival value is considered as safe and vice versa. The members of predator move to destroy the prey. A predator will be able to kill a herd only if the herd is within a predefined distance known as area of risk and the herd is less fit than the predator. Various steps involved in SHO algorithm are as follows:

5.1. Initialisation Phase

Select total number of population (N), maximum no of iteration (itrmax), upper bound x_j^{high} and lower bound x_j^{low} .

Initialise the set of population $A = \{a_1, a_2, ...a_N\}$

The positions of each member a_i is defined as:

$$a_{i,j}^{0} = x_j^{low} + rand(0,1).\left(x_j^{high} - x_j^{low}\right) \quad (23)$$

Where, i=1,2…. N and j=1,2…. n.
Break the total number of animals into two groups namely the prey or herd and the predator group.
No. of members in prey and predators groups are determined by

$$N_h = floor(N.rand(0.7,0.9))$$

$$N_p = N - N_h$$

Survival value of each animal is determined by

$$SV_{a_i} = \frac{f(a_i) - f_{best}}{f_{best} - f_{worst}} \quad (24)$$

Where, f_{best} and f_{worst} are evaluated as:

$$f_{best} = \min_{j\in\{0,1....k\}}\left(\left(\min_{i\in\{1,2....N\}}\left(f(a_i)\right)\right)_j\right)$$

$$f_{worst} = \max_{j\in\{0,1....k\}}\left(\left(\max_{i\in\{1,2....N\}}\left(f(a_i)\right)\right)_j\right)$$

5.2. Structurisation Phase

In the herd group, the member with minimum survival value is assigned as leader (h_L). The member having SV just above the leaders SV is named as the nearest neighbour (h_N).

$$h_L^K = \left(h_i^k \in H^k \middle| SV_{h_i^k} = \max_{j\in\{1,2,...,N_h\}}\left(SV_{h_j^k}\right)\right) \quad (25)$$

$$h_{N_j}^k = \left(h_j^k \in H^k, h_j^k \neq \left[h_i^k, h_L^k\right] \middle| SV_{h_j^k} > SV_{h_i^k}, r_{ij} = \min_{j\in\{1,2...,N_h\}}\left(\left\|h_i^k - h_j^k\right\|\right)\right) \quad (26)$$

As per the decision-making criteria regarding the change of position, the herd group members excluding leader is again divided into two subgroups called Herd followers and the Herd deserters.

$$H_F^k = \left\{h_i^k \neq h_L^k \middle| SV_{h_i^k} \geq rand(0,1)\right\} \quad (27)$$

$$H_D^k = \left\{h_i^k \neq h_L^k \middle| SV_{h_i^k} \geq rand(0,1)\right\} \quad (28)$$

Furthermore, Herd follower subgroup is divided into two parts depending on their survival value such as the Dominant herd members and the Subordinate herd members.

$$H_d^k = \left\{ h_i^k \in h_F^k \middle| SV_{h_i^k} \geq SV_{H_\mu^k} \right\} \quad (29)$$

$$H_s^k = \left\{ h_i^k \in h_F^k \middle| SV_{h_i^k} \geq SV_{H_\mu^k} \right\} \quad (30)$$

Where, $SV_{H_\mu^k} = \frac{\sum_{i=1}^{N_h} SV_{h_i^k}}{N_h}$

In each group herd and predator centre of mass is determined which represents the relatively safer and riskier positions respectively.

$$h_M^k = \frac{\sum_{i=1}^{N_h} SV_{h_i^k}.h_i^k}{\sum_{j=1}^{N_h} SV_{h_j^k}} \quad (31)$$

$$p_M^k = \frac{\sum_{i=1}^{Np} SV_{p_i^k}.p_i^k}{\sum_{j=1}^{N_p} SV_{p_j^k}} \quad (32)$$

5.3. Herd movement Phase

Each member of the herd group changes its position to escape from the predator attacking. This movement mainly depends on the attraction forces among the members of herd group and repulsion forces between members of herd and predators. The attraction force is given by:

$$\psi_{h_i,h_j} = SV_{h_j}.e^{-\left\|h_i-h_j\right\|^2} \tag{33}$$

The repulsion force is given by:

$$\varphi_{h_i,p_M} = -SV_{p_M}.e^{-\left\|h_i-p_M\right\|^2} \tag{34}$$

Herd's leader position is updated as:

$$h_L^{k+1} = \begin{Bmatrix} h_L^k + c^k \ \ if\ SV_{h_L^k} = 0 \\ h_L^k + s^k \ \ if\ SV_{h_L^k} > 0 \end{Bmatrix} \tag{35}$$

Where, $c^k = 2.\alpha.\phi^k_{h_L P_M}.(P_M^k - h_L^k)$, and $s^k = 2.\alpha.\psi^k_{h_L x_{best}}(x_{best}^k - h_L^k)$

Other members of the herd group update their position as:

$$h_i^{k+1} = \begin{Bmatrix} h_i^k + f_i^k & if\ h_i^k \in H_F^k \\ h_i^k + d_i^k & if\ h_i^k \in H_D^k \end{Bmatrix} \tag{36}$$

Where $f_i^k = \begin{Bmatrix} 2.\left(\beta.\psi^k_{h_i h_L}.\left(h_L^k - h_i^k\right) + \gamma.\psi^k_{h_i h_N}.\left(h_N^k - h_i^k\right)\right) & if\ h_i^k \in H_d^k \\ 2.\delta.\psi^k_{h_i h_M}.\left(h_M^k - h_i^k\right) & if\ h_i^k \in H_s^k \end{Bmatrix}$

and $d_i^k = 2.\left(\beta.\psi^k_{h_i h_{best}}.\left(x_{best}^k - h_i^k\right) + \gamma.\left(1 - SV_{h_i^k}\right)\hat{r}\right)$

5.4. Predator movement Phase

The members of the predator group change their position according to search likelihood between any one predator and one herd. Pursuit likelihood is given by:

$$P_{p_i h_j} = \frac{\omega_{p_i h_j}}{\sum_{m=1}^{N_h} \omega_{p_i h_M}} \tag{37}$$

Where $\omega_{p_i h_j} = \left(1 - SV_{h_j}\right).e^{-\left\|p_i - h_j\right\|^2}$

These members update their position as:

$$p_i^{k+1} = p_i^k + 2.\rho.\left(h_r^k - p_i^k\right) \tag{38}$$

5.5. Predation phase

Radius of domain of danger is calculated as:

$$R = \frac{\sum_{j=1}^{n} \left| x_j^{low} - x_j^{high} \right|}{2.n} \tag{39}$$

Threatened prey of a given predator is determined by

$$T_{p_i} = \left\{ h_j \in H \middle| SV_{h_j} < SV_{p_i}, \left\| p_i - h_j \right\| \le R, h_j \notin K \right\} \tag{40}$$

5.6. Restoration phase

To restore the size of herd group unaltered new members are generated by mating probability given by:

$$M_{h_j} = \frac{SV_{h_j}}{\sum_{(h_m \in M)} SV_{h_m}}, h_j \in M \tag{41}$$

Where, $M = \left\{ h_j \notin K \right\}$

A set of 'n' randomly selected individuals from the matrix M interchange their position by applying roulette selection method according to mating probability. With this a new solution is generated. The process is repeated until the stop criterion is met i.e., all the herd members are having higher survival value than that of the predator. The SHO algorithm is explained in a flowchart as depicted in Figure 5.

5.7. Pseudo code of SHO Algorithm

Step-1: Randomly generate the initial population.
Step-2: Classify the initial population into two groups namely Herd and Predator depending upon their performance.
Step-3: Select a member of the Herd group as the leader whose survival value is maximum and divide the remaining members of Herd group into two categories namely follower and deserter.
Step-4: Update the members of Herd and Predator groups.
Step-5: Determine the distance between the members of Predator and Herd groups to determine the domain of danger. If survival value of Predator is more than that of Herd and distance between them is less than the domain of domain of danger, then the Predator will kill the Herd.
Step-6: Randomly generate the solutions for the members of the Herd group which are killed by the Predator. Repeat steps 2-6 until the stopping criterion are met.

6. RESULTS AND DISCUSSION

6.1. Case-1: Transient study of the system

In this research work, a 3-equal area complex power system is addressed. The proposed model shown in Figure 1 is deployed in MATLAB-SIMULINK environment of version 2016(a).

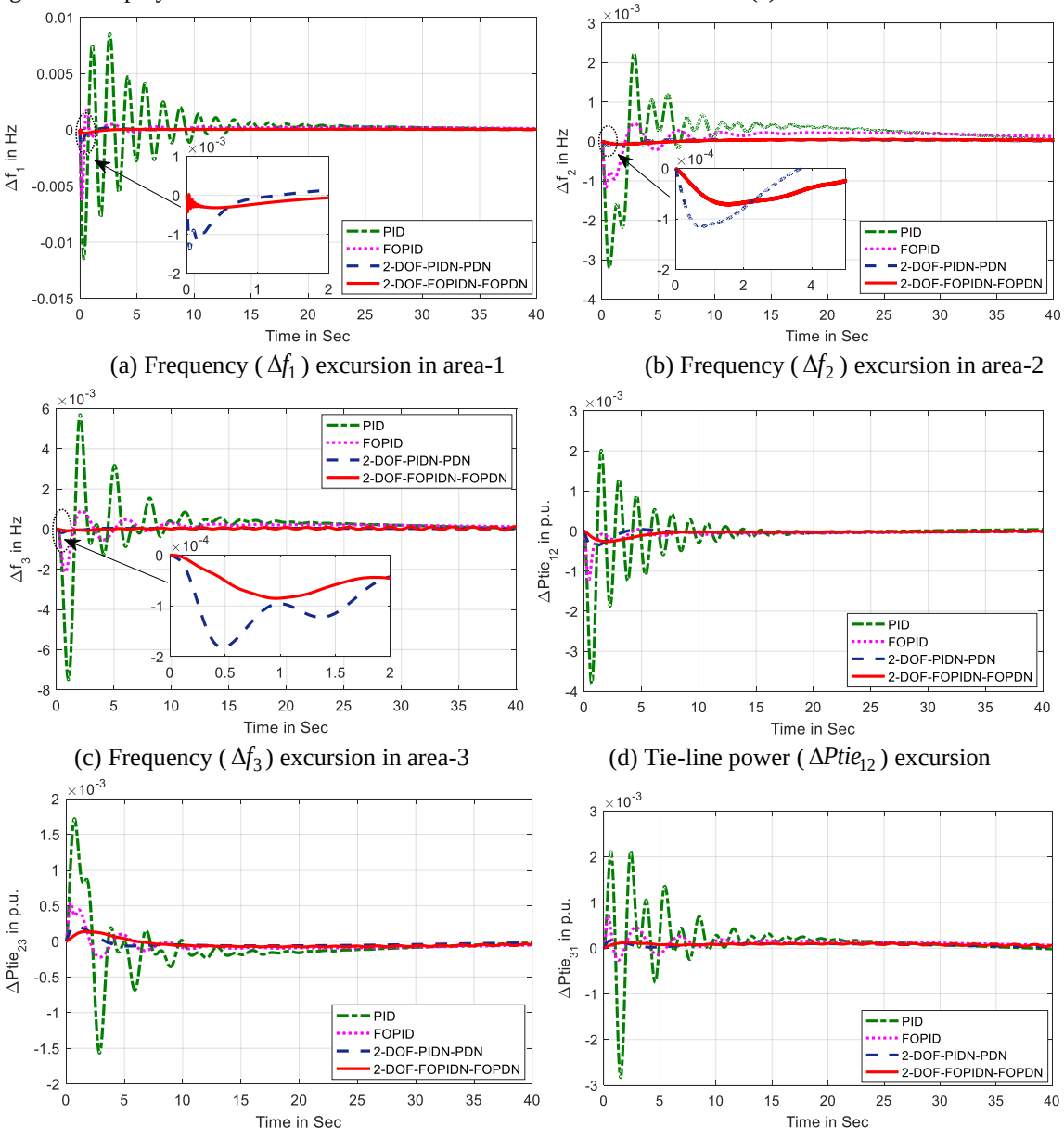

(a) Frequency (Δf_1) excursion in area-1
(b) Frequency (Δf_2) excursion in area-2
(c) Frequency (Δf_3) excursion in area-3
(d) Tie-line power ($\Delta Ptie_{12}$) excursion
(e) Tie-line power ($\Delta Ptie_{23}$) excursion
(f) Tie-line power ($\Delta Ptie_{31}$) excursion

Figure 5. Frequency and Tie-line power deviation curves.

Table 1. Optimal gains of controllers employed in the study.

Controllers	Gains	Controller:1	Controller:2	Controller:3	Controller:4	Controller:5
PID	G_p	2.4338	3.3000	2.0000	1.0000	1.0000
	G_i	4.2800	2.7500	1.5000	3.8301	0.3000
	G_d	0.7609	2.7807	1.0000	1.0000	0.3000
FOPID	G_p	1.2519	4.1434	4.5000	3.8216	4.0831
	G_i	4.5000	4.4482	4.5000	4.5000	4.5000
	G_d	0.0180	4.5000	4.5000	3.2359	4.5000
	σ	0.8000	0.8000	0.8000	0.8000	0.8000
	ζ	0.8000	0.8000	0.8000	0.4018	0.8000
2-DOFPIDN-PDN	G_{p1}	3.0000	3.0000	3.0000	3.0000	3.0000
	G_{i1}	3.0000	3.0000	3.0000	1.2560	2.9523
	G_{d1}	3.0000	2.2860	3.0000	1.2611	0.6556
	G_{p11}	1.6364	2.8099	2.3818	1.8230	2.9296
	G_{d11}	0.5186	1.0724	0.3330	3.0000	3.0000
	b_1	0.9500	0.9500	0.9492	0.9500	0.7987
	c_1	0.9500	0.9500	0.9500	0.9376	0.9500
	b_{11}	0.9500	0.9500	0.9500	0.9500	0.9500
	c_{11}	0.1023	0.9500	0.4584	0.7448	0.9500
	N_{f1}	116.3531	91.5053	70.7568	20.6028	196.2196
	N_{f11}	150.8212	200.000	158.3031	172.2966	119.1795
2-DOFFOPIDN-FOPDN	G_{p1}	3.0000	3.0000	2.8327	3.0000	1.8871
	G_{i1}	3.0000	3.0000	2.2520	1.3209	3.0000
	G_{d1}	2.0955	2.7158	3.0000	1.9477	2.5250
	G_{p11}	2.8287	2.2572	1.8918	3.0000	2.8772
	G_{d11}	2.7536	3.0000	2.6556	2.2946	3.0000
	b_1	0.9000	0.9000	0.9000	0.9000	0.4478
	c_1	0.9000	0.9000	0.9000	0.9000	0.8872
	b_{11}	0.9000	0.9000	0.9000	0.3186	0.9000
	c_{11}	0.5344	0.9000	0.9000	0.9000	0.9000
	σ	0.9000	0.2360	0.9000	0.9000	0.9000
	ζ_1	0.9000	0.8311	0.7995	0.9000	0.9000
	ζ_{11}	0.3275	0.5854	0.9000	0.8766	0.9000
	N_{f1}	67.0305	70.5405	157.3673	160.2716	189.8133
	N_{f11}	113.4389	26.5392	75.6793	28.9858	52.4699

To reduce the area control error (ACE), four different controllers e.g., PID, FOPID, 2-DOF-PIDN-PDN and 2-DOF-FOPIDN-FOPDN are demonstrated and again, to improve the dynamic performance, the parameters of these controllers are optimised by a novel SHO algorithm. The optimally designed parameters are depicted in the Table 1. The transient analysis is carried out by inserting a step load perturbation of 0.01 pu in area-1 at t=0 sec. The deviation in frequencies and tie-line powers in all the three areas with different proposed controllers are shown in the Figure 5. Undershoot (u_{sh}), overshoot (o_{sh}) and settling time (t_s) are the performance indicators of the dynamic response which are gathered in the Table 2. Inspecting the data presented in Table 2, it is found that the undershoot and overshoot of frequency and tie-line power deviation curves have been diminished abundantly in the presence of 2-DOF-FOPIDN-FOPDN controller. Also, it is observed that the fractional order influences the dynamic response produced by the integer-based controller acutely. The comparative study as in Table 2 shows that the 2-DOF-FOPIDN-FOPDN controller has outplayed the performance of other controllers. Simultaneously, it is noticed that the ITAE index has played a key role to augment the performance with ascertaining the gains of different controllers by minimising the errors. The observed ITAE values are 0.0217, 0.0202, 0.0065 and 0.0062 for PID, FOPID, 2-DOF-PIDN-

PDN and 2-DOF-FOPIDN-FOPDN controllers respectively. Hence, the designed 2-DOF-FOPIDN-FOPDN controller supersedes the other controllers in all the aspects.

Table 2. Undershoots, overshoots and settling times (with 0.00002 band) of frequency and (with 0.0001) tie-line power deviations.

Controllers	Indices	Δf_1	Δf_2	Δf_3	$\Delta ptie_{12}$	$\Delta ptie_{23}$	$\Delta ptie_{31}$	*ITAE*
PID	$o_{sh}\times10^{-3}$	8.5318	5.6988	2.2502	2.0160	1.7186	2.1201	
	$u_{sh}\times10^{-3}$	-11.4516	-3.2140	-7.4998	-3.8042	-1.5662	-2.8322	0.0217
	t_s in sec	25.148	32.54	27.52	16.263	20.235	22.081	
FOPID	$o_{sh}\times10^{-3}$	1.6788	0.9033	0.4503	0.0430	0.5404	0.7264	
	$u_{sh}\times10^{-3}$	-6.2632	-1.1654	-2.1552	-1.2657	-0.2239	-0.2657	0.0202
	t_s in sec	15.025	8.123	8.309	6.629	10.881	14.750	
2-DOFPIDN-PDN	$o_{sh}\times10^{-3}$	0.1549	0.0445	0.0440	0.0389	0.2043	0.1677	
	$u_{sh}\times10^{-3}$	-1.3673	-0.1155	-0.1819	-0.3719	-0.0655	0.0000	0.0065
	t_s in sec	0.715	3.548	1.628	2.834	2.272	2.201	
2-DOFFOPIDN-FOPDN	$o_{sh}\times10^{-3}$	**0.0512**	**0.0524**	**0.1201**	**0.0013**	**0.1378**	**0.1283**	
	$u_{sh}\times10^{-3}$	**-0.4267**	**-0.0722**	**-0.0853**	**-0.2623**	**-0.0790**	**0**	**0.0062**
	t_s in sec	**1.032**	**3.158**	**1.465**	**3.517**	**1.685**	**2.115**	

6.2. Case-2: Robustness study of the proposed controller against load variation

To examine the practicability of the proposed controller's performance against load variation, a randomly perturbed load as shown in Figure 6 (a) is introduced in area-1. Frequency deviation in area-1 and tie-line power interchanged between area-1 and area-2 are shown in Figures 6 (b) and 6 (c) respectively. From the response curves shown in figures 6 (b) and 6 (c), it is witnessed that the dynamic stability of the system is not vulnerable by the randomly varying load as the frequency and tie-line power deviations retained their respective nominal values within a short time. As the designed controller controls the alternation of tie line power and frequency smoothly with respect to a sudden load change, it can be believed that the robustness of the controller is proved.

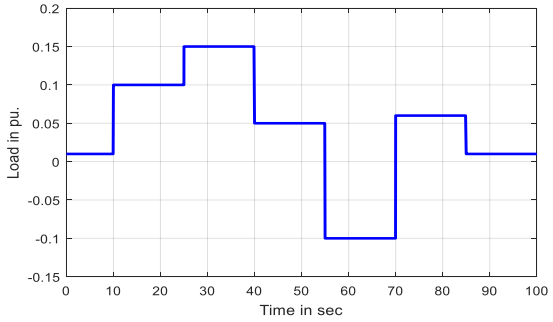

(a) Random load variation

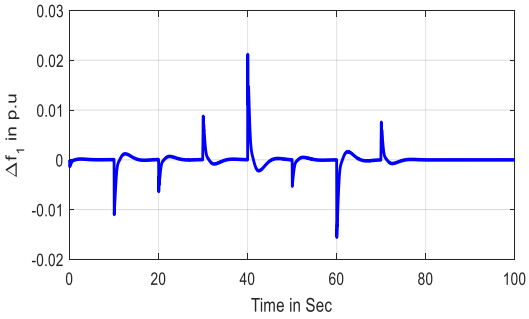

(b) Excursion of Δf_1 in area-1

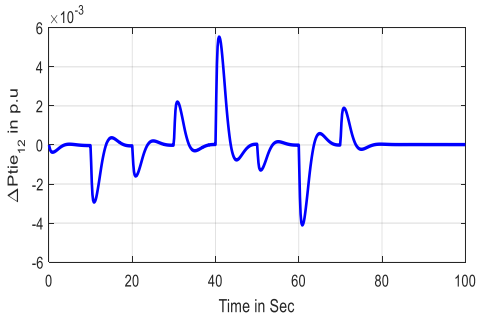

(c) Excursion of $\Delta Ptie_{12}$ in between area-1 and area-2

Figure 6. Frequency, and Tie-line power deviation against random load.

6.3. Case-3: Sensitivity analysis of the proposed controller against system's parametric variations:

During the normal/perturbed operation of the power system, there is a likelihood of deviation of system's parameter which reduces the stability or smooth operation of the power system. To tackle the aforementioned problem the controller has to be robust. So, to find the robustness of the proposed controller against system's parametric variations, some sensible parameters of the system are varied from -20 % to 20 % in steps of 10 % of their nominal values with 1 % step load disturbance in area-1. Undershoot, overshoot and settling time of the deviation in frequencies and tie-line power deviation due to parametric variations are provided in the Table 3 and Table 4 respectively, which reveals that the variation of specifications is quite negligible. As the proposed controller has controlled the system adequately without sacrificing its gains, it is concluded that the proficiency of the 2-DOF-FOPIDN-FOPDN is quite significant to deal with the parametric variations.

Table 3. Undershoots, overshoots and settling time of frequency alternation due to parametric variations.

Parameter	Parameter variation in %	Δf_1			Δf_2			Δf_3		
		u_{sh} $\times 10^{-3}$ in Hz	o_{sh} $\times 10^{-3}$ in Hz	t_s in sec	u_{sh} $\times 10^{-3}$ in Hz	o_{sh} $\times 10^{-3}$ in Hz	t_s in sec	u_{sh} $\times 10^{-3}$ in Hz	o_{sh} $\times 10^{-3}$ in Hz	t_s in sec
B	-20	-0.4395	0.0540	1.0331	-0.0774	0.0553	3.1601	-0.0920	0.1068	1.4631
	-10	-0.4329	0.0526	1.0322	-0.0747	0.0538	3.1595	-0.0886	0.1132	1.4589
	+10	-0.4207	0.0500	1.2990	-0.0699	0.0512	3.1576	-0.0822	0.1273	1.4597
	+20	-0.4150	0.0488	1.0300	-0.0676	0.0500	3.1498	-0.0792	0.1349	1.4656
R	-20	-0.4267	0.0521	1.0305	-0.0718	0.0533	3.1496	-0.0885	0.1535	1.4670
	-10	-0.4267	0.0516	1.0298	-0.0720	0.0528	3.1500	-0.0852	0.1337	1.4678
	+10	-0.4267	0.0510	1.0347	-0.0724	0.0522	3.1603	-0.0853	0.1103	1.4697
	+20	-0.4267	0.0508	1.0332	-0.0725	0.0520	3.1579	-0.0854	0.1029	1.4690
T_{12}	-20	-0.4268	0.0508	1.0354	-0.0644	0.0521	3.1498	-0.0840	0.1392	1.4598
	-10	-0.4267	0.0511	1.0318	-0.0685	0.0523	3.1499	-0.0798	0.1324	1.4670
	+10	-0.4266	0.0513	1.0306	-0.0757	0.0524	3.1603	-0.0903	0.1053	1.3959
	+20	-0.4266	0.0512	1.0299	-0.0789	0.0523	3.1604	-0.0948	0.0913	1..4590
K_{ps}	-20	-0.3842	0.0525	1.0298	-0.0724	0.0535	3.1580	-0.0894	0.1564	1.4587
	-10	-0.4059	0.0519	1.0323	-0.0723	0.0529	3.1587	-0.0860	0.1355	1.4665
	+10	-0.4467	0.0507	1.0308	-0.0723	0.0520	3.1579	-0.0849	0.1026	1.4635
	+20	-0.4663	0.0724	1.0297	-0.0724	0.0516	3.1651	-0.0849	0.0890	1.4624
T_{ps}	-20	-0.4758	0.0836	1.0298	-0.0725	0.0520	3.1558	-0.3395	0.3669	1.4558
	-10	-0.4489	0.0522	1.0308	-0.0723	0.0519	3.1495	-0.0848	0.0992	1.4676
	+10	-0.4078	0.0519	1.0289	-0.0723	0.0530	3.1487	-0.0860	0.1362	1.4684
	+20	-0.3916	0.0525	1.0340	-0.0724	0.0535	3.1576	-0.1013	0.1554	1.4685
K_r	-20	-0.4263	0.0476	1.0296	-0.0734	0.0490	3.1607	-0.0838	0.0464	1.4590
	-10	-0.4265	0.0474	1.0302	-0.0729	0.0488	3.1645	-0.0828	0.0463	1.4663
	+10	-0.4559	0.0423	1.0307	-0.0899	0.5011	3.1398	-0.0924	0.0845	1.4655
	+20	-0.4443	0.0744	1.0299	-0.0789	0.6083	3.1505	-0.0814	0.0476	1.4598
T_r	-20	-0.4267	0.0646	1.0325	-0.0725	0.0646	3.1499	-0.1040	0.3897	1.4586
	-10	-0.4267	0.0529	1.0338	-0.0723	0.0540	3.1667	-0.1068	0.1938	1.4628
	+10	-0.4267	0.0507	1.0298	-0.0721	0.0520	3.1578	-0.0849	0.0841	1.4681
	+20	-0.4267	0.0507	1.0335	-0.0721	0.0520	3.1550	-0.0847	0.0783	1.4576

Table 4. Undershoots, overshoots and settling time of tie-line power deviation due to parametric variations.

Parameters	Parameter variation in %	$\Delta Ptie_{12}$			$\Delta Ptie_{23}$			$\Delta Ptie_{31}$		
		u_{sh} $\times 10^{-3}$ in pu	o_{sh} $\times 10^{-3}$ in pu	t_s in sec	u_{sh} $\times 10^{-3}$ in pu	o_{sh} $\times 10^{-3}$ in pu	t_s in sec	u_{sh} $\times 10^{-3}$ in pu	o_{sh} $\times 10^{-3}$ in pu	t_s in sec
B	-20	-0.2671	0 .0000	3.5082	-0.0791	0.1411	1.6753	0.0000	0.1302	2.1105
	-10	-0.2647	0.0003	3.5071	-0.0790	0.1394	1.6678	0.0000	0.1293	2.1098
	+10	-0.2600	0.0023	3.5234	-0.0791	0.1362	1.6764	0.0000	0.1274	2.0997
	+20	-0.2578	0.0034	3.4992	-0.0792	0.1347	1.6842	0.0000	0.1264	2.0998
R	-20	-0.2619	0.0054	3.4986	-0.0803	0.1375	1.6843	0.0000	0.1282	2.2057
	-10	-0.2622	0.0030	3.5240	-0.0796	0.1377	1.6802	0.0000	0.1283	2.1060
	+10	-0.2625	0.0001	3.5142	-0.0786	0.1379	1.6756	0.0000	0.1284	2.1107
	+20	-0.2626	0.0000	3.4986	-0.0783	0.1379	1.6743	0.0000	0.1284	2.1150
T_{12}	-20	-0.2406	0.0020	3.4885	-0.0784	0.1235	1.6689	0.0000	0.1185	2.1156
	-10	-0.2522	0.0020	3.5205	-0.0788	0.1310	1.6658	0.0000	0.1238	2.1204
	+10	-0.2713	0.0002	3.5196	-0.0791	0.1440	1.6803	0.0000	0.1323	2.1181
	+20	-0.2792	0.0000	3.5086	-0.0791	0.1498	1.6798	0.0000	0.1359	2.1174
K_{ps}	-20	-0.2614	0.0057	3.5097	-0.0805	0.1385	1.6795	0.0000	0.1279	2.1098
	-10	-0.2618	0.0048	3.5308	-0.0798	0.1380	1.6880	0.0000	0.1281	2.0996
	+10	-0.2630	0.0000	3.5081	-0.0784	0.1377	1.6785	0.0000	0.1286	2.1211
	+20	-0.2639	0.0000	3.4995	-0.0778	0.1378	1.6587	0.0000	0.1289	2.1186

T_{ps}	-20	-0.2644	0.0031	3.4988	-0.0780	0.1379	1.6591	0.0000	0.1290	2.1085
	-10	-0.2631	0.0000	3.5025	-0.0782	0.1377	1.6779	0.0000	0.1286	2.1068
	+10	-0.2618	0.0048	3.4894	-0.0798	0.1380	1.6759	0.0000	0.1281	2.1098
	+20	-0.2615	0.0052	3.5129	-0.0805	0.1383	1.6587	0.0000	0.1280	2.1149
K_r	-20	-0.2613	0.0000	3.5054	-0.0745	0.1411	1.6649	0.0000	0.1226	2.1147
	-10	-0.2615	0.0000	3.4987	-0.0741	0.1396	1.6758	0.0000	0.1250	2.1147
	+10	-0.2754	0.0065	3.5182	-0.0847	0.1346	1.6815	-0.0012	0.1604	2.1099
	-20	-0.2586	0.0057	3.5190	-0.0843	0.1859	1.6840	-0.0025	0.1793	2.1050
T_r	-20	-0.2628	0.0043	3.5210	-0.0942	0.1381	1.6756	-0.0468	0.1530	2.1147
	-10	-0.2625	0.0119	3.5008	-0.0806	0.1379	1.6870	0.0000	0.1287	2.1150
	+10	-0.2622	0.0000	3.5204	-0.0788	0.1377	1.6846	0.0000	0.1280	2.1145
	-20	-0.2621	0.0000	3.5169	-0.0789	0.1376	1.6794	0.0000	0.1279	2..1152

7. EXTENDED WORK

To support the potential of SHO algorithm as well as, the proposed 2-DOF-FOPIDN-FOPDN controller, another model is taken into consideration. This model is a 2-area system in which a FO based controller is employed to study the LFC. The FO controllers are optimised by the path finder algorithm (PFA). The detailed analysis is described below.

7.1. Power system Model

A two equal area interconnected power system with diversified sources is considered to prove the efficacy of the recommended controller as well as, optimisation technique. The system is shown in Figure 7 and its parameters are taken from [34]. To obtain the frequency stability of the system, different controllers such as PID, TID, FOTID, 2-DOF-PIDN-PDN and 2-DOF-FOPIDN-FOPDN are deployed in this work. Following the same objective function and same procedure, the step response of the system is evaluated.

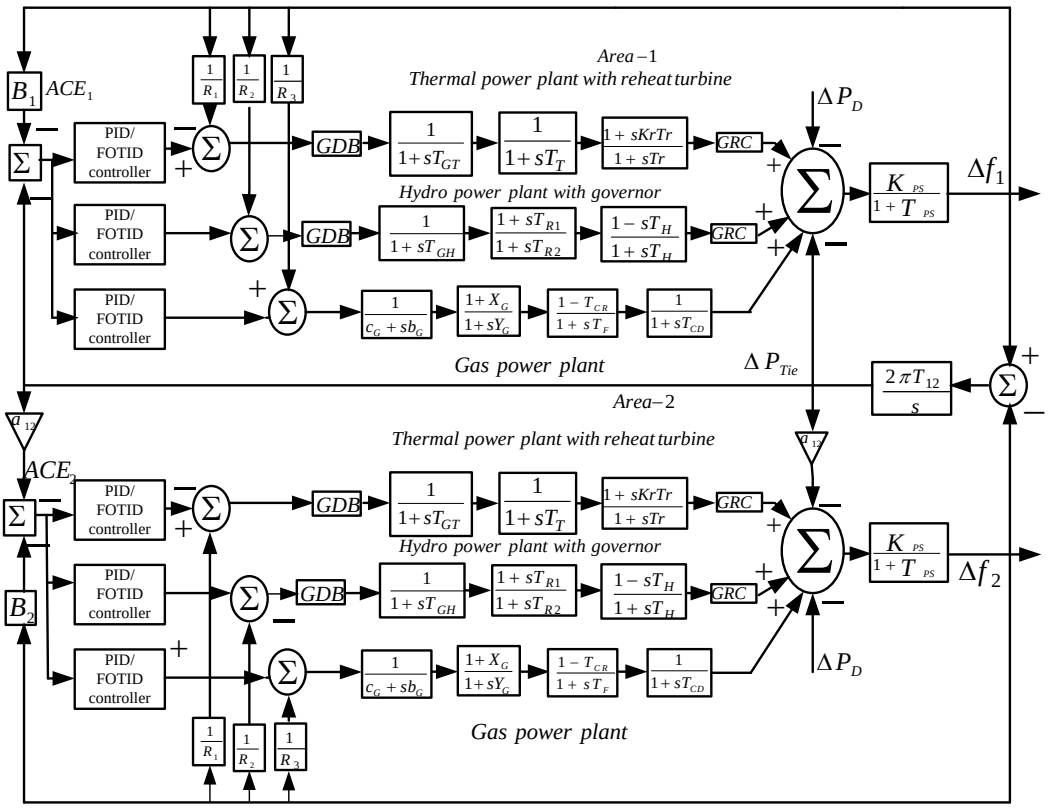

Figure 7. Two area multi-source system

7.2. Result analysis

In this extended work, stability analysis of the given two area system is carried out by injecting a SLP of 0.01 p.u. to the first area at t=0 sec. Various controllers are used to reduce the area control error of the system by which frequency and tie-line power deviation can be minimised. The gains of the controllers are tuned by the selfish herd optimisation technique. The frequency and tie-line power deviations are shown in the Figure

8. The performance indices are given in the Table 5. The result is compared with the recently published work [34]. To prove the performance of the optimisation technique the result of both PID and TID controller tuned with SHO technique is compared with that of PFA tuned PID and TID controllers. Figure 8 indicates that the proposed SHO algorithm based PID and TID works better than the PFA based PID and TID controllers. Again, the result of the proposed SHO tuned 2-DOF-FOPIDN-FOPDN controller is compared with the result of FOTID controller tuned by the same SHO. Figure 8 witnesses that the SHO-2-DOF-FOPIDN-FOPDN controller has outperformed the SHO-FOTID controller. The transient specifications are gathered in Table 5. The data in Table 5 shows that the SHO based controllers have curtailed the undershoot, overshoot and settling time significantly. So, from the dynamic response as in Figure 8 and transient specifications as in Table 5, it quite evident that the proposed SHO based 2-DOF-FOPIDN-FOPDN controller has outplayed the other employed controllers designed by SHO and/or PFA algorithms.

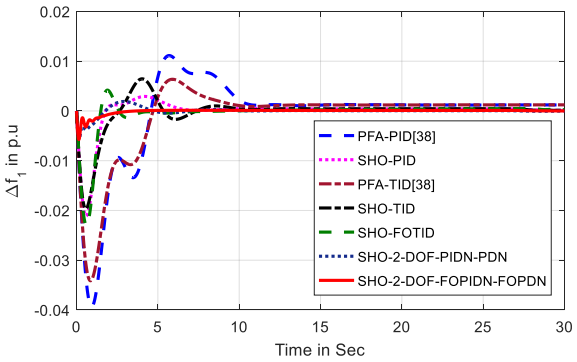

(a) Frequency (Δf_1) excursion in area-1

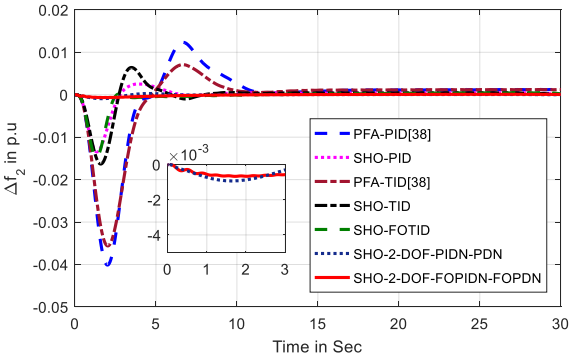

(b) Frequency (Δf_2) excursion in area-2

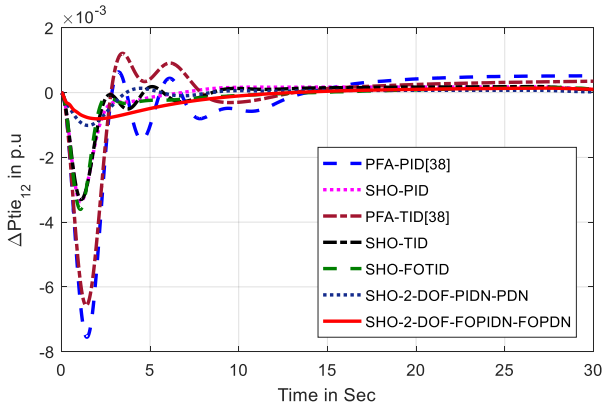

(c) Tie-line power ($\Delta Ptie_{12}$) excursion

Figure 9. Frequency and Tie-line power deviation curves.

Table 5. Undershoots, overshoots and settling times (with 0.0002 band) of frequency and tie-line power deviations

Optimization technique	Δf_1			Δf_2			$\Delta ptie_{12}$		
Performance Indices	$u_{sh}\times10^{-3}$	$o_{sh}\times10^{-3}$	t_s in sec (0.2%)	$u_{sh}\times10^{-3}$	$o_{sh}\times10^{-3}$	t_s in sec (0.05%)	$u_{sh}\times10^{-3}$	$o_{sh}\times10^{-3}$	t_s in sec (0.2%)
PFA-PID	-39.3467	11.1370	29.14	-40.1232	12.3527	28.45	-7.5547	0.6443	23.65
SHO-PID	-21.1147	2.9176	6.918	-13.4536	2.5311	7.631	-3.3717	0.1757	4.559
PFA-TID	-28.3836	5.5087	26.80	-29.4650	5.9029	26.73	-5.4589	1.0222	21.95
SHO-TID	-19.6792	6.4594	11.64	-16.4138	6.4138	11.78	-3.3011	0.1857	7.46
SHO- FOTID	-22.9774	4.1906	6.743	-14.6642	0.5036	8.04	-3.6074	0.1630	6.882
SHO-2DOF-PIDN-PDN	-5.6902	1.906	6.48	-0.9326	0.2891	5.305	-1.0134	0.1394	3.204
SHO-2DOF-FOPIDN-FOPDN	**-5.6482**	**0.1346**	**2.83**	**-0.6679**	**0.1113**	6.684	**-0.8087**	**0.1388**	8.201

8. CONCLUSION

The 3-area power system comprising six different diversified sources is simulated in MATLAB/SIMULINK environment. The system behaviour with different nonlinearities are evaluated by the help of PID, FOPID, 2-DOF-PIDN-PDN and 2-DOF-FOPIDN-FOPDN controllers. The proposed 2-DOF-

FOPIDN-FOPDN controller produces better result in comparison to other controllers in terms of settling time, overshoot and undershoot. The robustness of the controller and optimisation technique is proved by comparing its result with PFA tuned TID and FOTID controllers. The stability of the system as well as the robustness of the proposed controller is preserved with respect to an awake of load perturbation and parametric variations. The proficient, and robust controller is well enough to supply the quality power to the end users. Further, the performance of the system can be improved by the utilising some intelligent controllers with injecting stochastic load in all areas, in future.

APPENDIX A

$K_{ps} = 120$, $T_{ps} = 20s$, $R_x = R_y = R_z = 2.4$, $B_1 = B_2 = B_3 = 0.425$, $T_{12} = T_{23} = T_{31} = 0.0707$,

$a_{12} = a_{13} = a_{23} = -1$ **Thermal Units:**

$T_{g1} = 0.2\,s$, $T_t = 0.3s$, $T_r = 10\,s$, $K_r = 0.333$, $N_1 = 0.8$, $N_2 = -0.2$, $K_1 = 0.85$, $K_2 = 0.095$, $K_3 = 0.92$,

$c_B = 200$, $K_{ib} = 0.5$, $T_{ib} = 26\,s$, $T_{rb} = 69\,s$, $T_D = 0$, $T_F = 10\,s$, $T_t = 0.3\,s$.

Hydro Units:

$T_{g2} = 48.7\,s$, $T_1 = 0.513s$, $T_2 = 10\,s$, $T_w = 1s$.

Gas Unit:

$C_{GS} = 1$, $B_{GS} = 0.05$, $X_{GS} = 0.6$, $Y_{GS} = 1$, $T_{CR} = 0.01\,s$, $T_{FR} = 0.23\,s$, $T_{CD} = 0.2\,s$.

Wind Farm & Diesel Unit:

$k_2 = 1.25$, $k_3 = 1.4$, $T_{p1} = 0.6\,s$, $T_{p2} = 0.041s$, $k_{diesel} = 16.5$.

Solar Unit:

$K_{PV} = 4.64$, $T_{PV} = 0.054s$

APPENDIX B

$K_{PS} = 68.95$, $T_{PS} = 11.49s$

Thermal Units:

$T_{g1} = 0.08\,s$, $T_t = 0.3\,s$, $T_r = 10\,s$, $K_r = 0.3$, $N_1 = 0.8$, $N_2 = -0.2$

Hydro Units:

$T_{g2} = 28.75\,s$, $T_1 = 0.2s$, $T_2 = 5\,s$, $T_w = 1s$.

Gas Unit:

$C_{GS} = 1$, $B_{GS} = 0.05$, $X_{GS} = 0.6$, $Y_{GS} = 1$, $T_{CR} = 0.01\,s$, $T_{FR} = 0.23\,s$, $T_{CD} = 0.2\,s$.

REFERENCES

[1] M.F. Hassan, A.A. Abouelsoud, H.M. Soliman, "Constrained load-frequency control," Electric Power Components and Systems, vol. 36(3), 2008, pp.266-79.

[2] Ramakrishna, K. S. S., Bhatti T.S, "Automatic generation control of single area power system with multi-source power generation" Proceedings of the Institution of Mechanical Engineers, Part A: Journal of Power and Energy 222(1), 2008, pp.1-11.

[3] Dabur P., Yadav N. K., Avtar R, "Matlab design and simulation of AGC and AVR for single area power system with fuzzy logic control," International Journal of Soft Computing and Engineering, 1(6). 2012, pp. 44-49.

[4] Kothari M.L, Nanda J, Kothari D.P, Das D, "Discrete-mode automatic generation control of a two-area reheat thermal system with new area control error," IEEE Transactions on power systems 4(2), pp.730-738.

[5] Bhise G.G, Kothari M.L, Nanda J, "Optimum selection of hydro governor parameters for automatic generation control of a hydrothermal system," In Advances in Power System Control, Operation and Management, 1993. APSCOM-93., 2nd International Conference. pp. 910-915.

[6] Subha S, "Load frequency control with fuzzy logic controller considering governor dead band and generation rate constraint non-linearities," World Appl. Sci. Journal 29(8), 2014, pp.1059-66.

[7] Tripathy S.C, Balasubramanian R, Nair P, "Effect of superconducting magnetic energy storage on automatic generation control considering governor dead band and boiler dynamics," IEEE Transactions on Power systems 7(3), 1992, pp.1266-73.

[8] Gozde H, Taplamacioglu M.C, "Automatic generation control application with craziness-based particle swarm optimization in a thermal power system," Int J Electrical Power & Energy Syst,33(1), 2011, pp. 8-16.

[9] Guha D, Roy P.K, Banerjee S, "Symbiotic organism search algorithm applied to load frequency control of multi-area power system," Energy Systems. 9(2), 2018, pp. 439-468.
[10] Nanda J, Mishra S, Saikia L.C, "Maiden application of bacterial foraging-based optimization technique in multiarea automatic generation control," IEEE Transactions on power systems ,24(2), 2009, pp.602-609.
[11] Elgerd O.I, Fosha C.E, "Optimum megawatt-frequency control of multiarea electric energy systems," IEEE Transactions on Power Apparatus and Systems, 4, 1970, pp. 556-563.
[12] Parmar K, Singh P, "PSO based PI Controller for the LFC System of an Interconnected Power System," International journal of computer applications, 2014, pp.88-107.
[13] Ali, E. S., S. M. Abd-Elazim, "FOA based design of PID controller for two area load frequency control with nonlinearities," International Journal of Electrical Power & Energy Systems, 51, 2013, pp. 224-231.
[14] Sahu R.K, Panda S, Sekhar G.C, "A novel hybrid PSO-PS optimized fuzzy PI controller for AGC in multi area interconnected power systems," Int J Electrical Power & Energy Syst, 64, 2015, pp.880-893.
[15] Sahu B.K, Pati S, Mohanty P.K, Panda S, "Teaching–learning based optimization algorithm based fuzzy-PID controller for automatic generation control of multi-area power system," Applied Soft Computing 27, 2015, pp. 240-249.
[16] Sahoo, S., Jena, N. K., Dei, G., Sahu, B. K., "Self-adaptive fuzzy-PID controller for AGC study in deregulated Power System," Indonesian Journal of Electrical Engineering and Informatics (IJEEI), 7(4), 2019, pp.650-663.
[17] Sahu R.K, Panda S, Rout U.K, "DE optimized parallel 2-DOF PID controller for load frequency control of power system with governor dead-band nonlinearity. Int J Electrical Power & Energy Syst, 49, 2013 pp.19-33.
[18] Nayak J.R., Shaw B, Sahu B.K, "Novel application of optimal fuzzy-adaptive symbiotic organism search-based two-degree-of-freedom fuzzy proportional integral derivative controller for automatic generation control study," International Transactions on Electrical Energy Systems, 2020.
[19] Morsali J, Zare K, Hagh MT, "Applying fractional order PID to design TCSC-based damping controller in coordination with automatic generation control of interconnected multi-source power system," Engineering Science and Technology, an International Journal.20(1), (2013) 1-7.
[20] Farook S, Sangmeswara P, Raju, "Decentralized fractional order PID controller for AGC in a multi area deregulated power system," International Journal of Advances in Electrical and Electronics Engineering 1(3), 2013, pp. 317-332.
[21] Dash P, Saikia L C, Sinha N (2016) Flower pollination algorithm optimized PI-PD cascade controller in automatic generation control of a multi-area power system. Int J Electric Power & Energy Syst 82:19-28.
[22] Debnath, M. K, Jena. T, Mallick R. K, "Novel PD-PID cascaded controller for automatic generation control of a multi-area interconnected power system optimized by grey wolf optimization (GWO)," IEEE 1st International Conference on Power Electronics, Intelligent Control and Energy Systems (ICPEICES). IEEE, 2016.
[23] Saha A, Saikia L.C, "Utilisation of ultra-capacitor in load frequency control under restructured STPP-thermal power systems using WOA optimised PIDN-FOPD controller," IET Generation, Transmission & Distribution 11(13), 2017, pp. 3318-3331.
[24] Tasnin W, Saikia L.C, "Performance comparison of several energy storage devices in deregulated AGC of a multi-area system incorporating geothermal power plant," IET Renewable Power Generation 12(7). 2018, pp.761-72.
[25] Arya Y, Kumar N, Dahiya P., Sharma, G., Çelik, E., Dhundhara S., Sharma, M, "Cascade-IλDμN controller design for AGC of thermal and hydro-thermal power systems integrated with renewable energy sources." IET Renewable Power Generation, 15(3), 2021, pp. 504-520.
[26] Prakash A, Murali S, Shankar R, Bhusan R, "HVDC tie-link modeling for restructured AGC using a novel fractional order cascade controller," Electric Power Systems Research, 170, 2019, pp. 244-258.
[27] Sitikantha D, Sahu B.K and Mohanty P.K, "Implementation of WOA-Based 2DOF-FOPID Controller for AGC of Interconnected Power System," Computational Intelligence in Pattern Recognition. Springer, Singapore, 2020, pp. 909-920.
[28] Raj U, Shankar R, "Deregulated Automatic Generation Control using Novel Opposition-based Interactive Search Algorithm Cascade Controller Including Distributed Generation and Electric Vehicle," Iranian Journal of Science and Technology, Transactions of Electrical Engineering, 2020, pp. 1-19.
[29] Jena, N. K, Sahoo S, Sahu B.K, "Fractional order cascaded controller for AGC study in power system with PV and diesel generating units," Journal of Interdisciplinary Mathematics 23(2), 2020, pp. 425-434.
[30] Sharma Y, Saikia L.C (2015) Automatic generation control of a multi-area ST–Thermal power system using Grey Wolf Optimizer algorithm based classical controllers. Int J Electric Power & Energy Syst 73:853-62.
[31] Fausto F, Cuevas E, Valdivia A, González A, "A global optimization algorithm inspired in the behavior of selfish herds," Biosystems, 160, 2017, pp.39-55.
[32] Abdel-Magid Y L, Abido M A, "AGC tuning of interconnected reheat thermal systems with particle swarm optimization," In Electronics, Circuits and Systems, 2003. ICECS 2003. Proceedings of the 2003 10th IEEE International Conference 14 (1), (2003), pp.376-379.
[33] Gozde H, Taplamacioglu M.C, Kocaarslan I, "Comparative performance analysis of Artificial Bee Colony algorithm in automatic generation control for interconnected reheat thermal power system," Int J Electric Power & Energy Syst, 42(1), 2012, pp.167-78.
[34] Priyadarshani S, Subhashini K.R, Satapathy J.K, "Pathfinder algorithm optimized fractional order tilt-integral-derivative (FOTID) controller for automatic generation control of multi-source power system," Microsystem Technologies, 27(1), 2021, pp. 23-35.
[35] Morsali J, Zare K, Hagh M.T, "MGSO optimised TID-based GCSC damping controller in coordination with AGC for diverse-GENCOs multi-DISCOs power system with considering GDB and GRC non-linearity effects," IET Generation, Transmission & Distribution 11(1), 2017, pp.193-208.

[36] Behera A, Panigrahi T.K., Pati S.S, Ghatak S., Ramasubbareddy S., Gandomi A.H, "A hybrid evolutionary algorithm for stability analysis of 2-area multi-non-conventional system with communication delay and energy storage," International Journal of Electrical Power & Energy Systems, 130,2021, pp. 1068-23.
[37] Podlubny I., "Fractional-order systems and PI/sup/spl lambda//D/sup/spl mu//-controllers," IEEE Transactions on automatic control, 44(1), 1999, pp.208-14.
[38] Oustaloup A, Levron F, Mathieu B, Nanot F.M, "Frequency-band complex non integer differentiator: characterization and synthesis," IEEE Transactions on Circuits and Systems I: Fundamental Theory and Applications 47(1), 2000, pp. 25-39.
[39] Pan I, Das S, "Fractional order fuzzy control of hybrid power system with renewable generation using chaotic PSO," ISA transactions 62, 2016, pp.19–29.